TOPOLOGICAL DERIVATIVE-BASED TOPOLOGY OPTIMIZATION OF STRUCTURES SUBJECT TO DESIGN-DEPENDENT HYDROSTATIC PRESSURE LOADING

M. XAVIER AND A.A. NOVOTNY

Abstract. In this paper the topological derivative concept is applied in the context of compliance topology optimization of structures subject to design-dependent hydrostatic pressure loading under volume constraint. The topological derivative represents the first term of the asymptotic expansion of a given shape functional with respect to the small parameter which measures the size of singular domain perturbations, such as holes, inclusions, source-terms and cracks. In particular, the topological asymptotic expansion of the total potential energy associated with plane stress or plane strain linear elasticity, taking into account the nucleation of a circular inclusion with non-homogeneous transmission condition on its boundary, is rigorously developed. Physically, there is a hydrostatic pressure acting on the interface of the topological perturbation, allowing to naturally deal with loading-dependent structural topology optimization. The obtained result is used in a topology optimization algorithm based on the associated topological derivative together with a level-set domain representation method. Finally, some numerical examples are presented, showing the influence of the hydrostatic pressure on the topology of the structure.

1. Introduction

The topological derivative measures the sensitivity of a given shape functional with respect to an infinitesimal singular domain perturbation, such as the insertion of holes, inclusions, source-terms or even cracks. The topological derivative was rigorously introduced by Sokołowski and Żochowski (1999). Since then, this relatively new concept has proved to be useful in the treatment of a wide range of physical and engineering problems such as topology optimization, inverse problems, image processing, multiscale material design, fracture mechanics sensitivity analysis and damage evolution modeling. For a comprehensive account on the topological derivative concept and its applications see, for instance, the book by Novotny and Sokołowski (2013).

In this work the topological derivative concept is applied in the context of topology optimization of structures subject to design-dependent hydrostatic pressure loading. The basic idea consists in minimizing the structural compliance under volume constraint. In particular, the topological asymptotic expansion of the total potential energy associated with plane stress or plane strain linear elasticity, taking into account the nucleation of a circular inclusion with non-homogeneous transmission condition on its boundary, is rigorously developed. Physically, there is a hydrostatic pressure acting on the interface of the topological perturbation, allowing to naturally deal with loading-dependent structural topology optimization. The obtained result is used in a topology optimization algorithm based on the associated topological derivative together with a level-set domain representation method as proposed by Amstutz and Andrä (2006). Finally, some numerical examples are presented, showing the influence of the hydrostatic pressure on the topology of the structure.

Topology optimization of structures subject to design-dependent pressure loading has been already treated in the literature by using standard approaches, such as SIMP (Hammer and Olhoff, 2000; Chen and Kikuchi, 2001; Sigmund and Clausen, 2007; Gao and Zhang, 2009; Lee and Martins, 2012; Wang et al., 2016) or level-set methods (Q. Xia and Shi, 2015). See alternative formulations proposed by Fuchs and Shemesh (2004) and Du and Olhoff. (2004a,b). We also note that the topological derivative with respect to the nucleation of holes or inclusions endowed with homogeneous conditions is known in the literature. Its applications in the context of topology optimization of structures can be found in many references. See, for instance, the works by Amstutz and Novotny (2010); Céa et al. (2000); Garreau et al. (2001); Norato et al. (2007). In addition, topological asymptotic analysis taking into account non-homogeneous conditions on the boundary of the holes has been derived by Novotny et al. (2003), for instance. On the other hand, there are no results concerning non-homogeneous transmission conditions on

Key words and phrases. structural topology optimization, design-dependent loading, hydrostatic pressure, topological derivatives.

the interface of the topological perturbation. Therefore, the topological asymptotic analysis with respect to the nucleation of an inclusion submitted to hydrostatic pressure is new and represents the main contribution of this work.

The paper is organized as follows. The topological derivative concept is introduced in the beginning of Section 2. The mechanical problem we are dealing with is presented in Section 2.1. In Section 2.2 we provide arguments concerning existence of the associated topological derivative. Its closed form is rigorously derived in Section 2.3. Then, some numerical experiments are driven in Section 3. Finally, the concluding remarks are presented in Section 4.

2. Topological Sensitivity Analysis

Let us consider an open and bounded domain $\mathcal{D} \subset \mathbb{R}^2$ with a Lipschitz boundary $\partial\mathcal{D}$, which is subject to a nonsmooth perturbation confined in a small region $B_\varepsilon(\hat{x})$ of size ε centered at an arbitrary point $\hat{x} \in \mathcal{D}$, as shown in the sketch of Figure 1. We introduce a characteristic function $x \mapsto \chi(x)$, $x \in \mathbb{R}^2$, associated with the unperturbed domain, namely $\chi = \mathbb{1}_{\mathcal{D}}$, such that:

$$|\mathcal{D}| = \int_{\mathbb{R}^2} \chi, \tag{2.1}$$

where $|\mathcal{D}|$ is the Lebesgue's measure of $\mathcal{D}$. Then, we define a characteristic function associated with the topologically perturbed domain of the form $x \mapsto \chi_\varepsilon(\hat{x}; x)$, $x \in \mathbb{R}^2$. In the case of a perforation, for example, $\chi_\varepsilon(\hat{x}) = \mathbb{1}_{\mathcal{D}} - \mathbb{1}_{B_\varepsilon(\hat{x})}$, and the perforated domain is obtained as $\mathcal{D}_\varepsilon(\hat{x}) = \mathcal{D} \setminus \overline{B_\varepsilon(\hat{x})}$. Then, we assume that a given shape functional $\psi(\chi_\varepsilon(\hat{x}))$, associated with the topologically perturbed domain, admits the following topological asymptotic expansion:

$$\psi(\chi_\varepsilon(\hat{x})) = \psi(\chi) + f(\varepsilon) D_T\psi(\hat{x}) + o(f(\varepsilon)), \tag{2.2}$$

where $\psi(\chi)$ is the shape functional associated to the original domain, that is, without perturbation, $f(\varepsilon)$ is a positive function such that $f(\varepsilon) \to 0$ when $\varepsilon \to 0$ and $o(f(\varepsilon))$ is the remainder. The function $\hat{x} \mapsto D_T\psi(\hat{x})$ is called the topological derivative of ψ at $\hat{x}$. Therefore, this derivative can be seen as a first order correction of $\psi(\chi_\varepsilon(\hat{x}))$. In fact, after rearranging (2.2) we have

$$\frac{\psi(\chi_\varepsilon(\hat{x})) - \psi(\chi)}{f(\varepsilon)} = D_T\psi(\hat{x}) + \frac{o(f(\varepsilon))}{f(\varepsilon)}. \tag{2.3}$$

The limit passage $\varepsilon \to 0$ in the above expression leads to the general definition for the topological derivative, namely

$$D_T\psi(\hat{x}) = \lim_{\varepsilon \to 0} \frac{\psi(\chi_\varepsilon(\hat{x})) - \psi(\chi(x))}{f(\varepsilon)}. \tag{2.4}$$

It is worth to mention that the topological derivative is defined through a limit passage when the small parameter governing the size of the topological perturbation goes to zero (2.4). However, it can be used as a steepest-descent direction in an optimization process like in any method based on the gradient of the cost functional.

2.1. Problem Statement.

Let us decompose $\mathcal{D}$ into two subdomains $\omega \subset \mathcal{D}$ and $\mathcal{D} \setminus \overline{\omega}$. The subdomain $\Omega := \mathcal{D} \setminus \overline{\omega}$ represents an elastic and deformable region, while ω is filled by a very compliant material. In addition, the region ω is subject to a hydrostatic pressure. The minimization problem we are dealing with can be defined in the following way:

$$\begin{cases} \underset{\Omega \subset \mathcal{D}}{\text{Minimize}} & -\mathcal{J}_\chi(u) \\ \text{subject to} & |\Omega| \leq M, \end{cases} \tag{2.5}$$

where the shape functional $\mathcal{J}_\chi(u)$ is given by the total potential energy of the system, $|\Omega|$ is the Lebesgue's measure of Ω and M represents the required volume at the end of the minimization process. The volume constraint is trivially imposed by using a linear penalization approach. For more elaborate strategies, see for instance the work by Campeão et al. (2014). In particular, the constrained optimization problem (2.5) is replaced by the following unconstrained optimization problem:

$$\underset{\Omega \subset \mathcal{D}}{\text{Minimize}}\, \mathcal{F}_\chi(u) = -\mathcal{J}_\chi(u) + m\,|\Omega|\,, \tag{2.6}$$

where $m > 0$ is a fixed multiplier used to impose the volume constraint of elastic material. This means that the shape functional to be minimized is the strain energy stored into the structure with a volume constraint. In other words, the total potential energy $\mathcal{J}_\chi(u)$ is written as:

$$\mathcal{J}_\chi(u) = \frac{1}{2}\int_{\mathcal{D}} \sigma(u) \cdot \nabla u^s - \int_{\Gamma_N} \overline{q} \cdot u - \int_{\omega} p\,\mathrm{div}(u), \tag{2.7}$$

where the vector function u is the solution of the following variational problem: Find $u \in \mathcal{U}$, such that

$$\int_{\mathcal{D}} \sigma(u) \cdot \nabla \eta^s = \int_{\Gamma_N} \overline{q} \cdot \eta + \int_{\omega} p\,\mathrm{div}(\eta),\ \forall \eta \in \mathcal{V}. \tag{2.8}$$

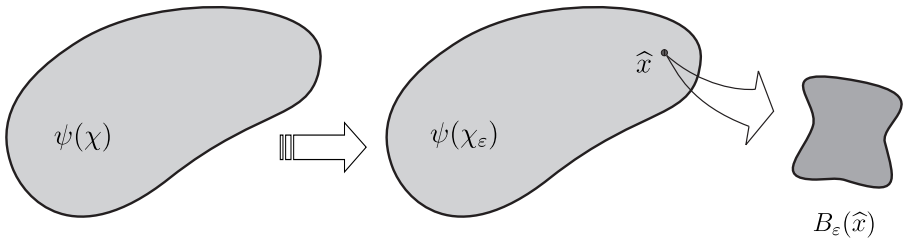

FIGURE 1. The topological derivative concept.

Some terms in the above variational equation require explanation. The Cauchy stress tensor is given by

$$\sigma(u) = \rho\mathbb{C}\nabla u^s, \text{ with } \nabla u^s = \frac{1}{2}(\nabla u + \nabla u^\top), \quad (2.9)$$

where the parameter ρ is defined as

$$\rho = \rho(x) := \begin{cases} 1 & \text{if } x \in \Omega, \\ \rho_0 & \text{if } x \in \omega, \end{cases} \quad (2.10)$$

with $0 < \rho_0 \ll 1$ used to mimic the voids. The elasticity tensor $\mathbb{C}$ is given by

$$\mathbb{C} = 2\mu\mathbb{I} + \lambda \mathrm{I} \otimes \mathrm{I}, \quad (2.11)$$

where I and $\mathbb{I}$ are respectively second and fourth identity tensors, μ and λ are the Lamé's coefficients, both constants in all domain. In particular, we have:

$$\mu = \frac{E}{2(1+\nu)}, \ \lambda = \frac{\nu E}{1-\nu^2} \text{ and } \lambda^* = \lambda\frac{1-\nu}{1-2\nu}, \quad (2.12)$$

where λ and λ^* are associated with plane strain and plane stress assumptions, respectively. In addition, E is the Young's modulus and ν the Poisson's ratio. The set $\mathcal{U}$ and the space $\mathcal{V}$ are respectively defined as:

$$\mathcal{U} := \left\{\varphi \in H^1(\mathcal{D}) : \varphi_{|\Gamma_D} = \overline{u}\right\}, \quad (2.13)$$

$$\mathcal{V} := \left\{\varphi \in H^1(\mathcal{D}) : \varphi_{|\Gamma_D} = 0\right\}. \quad (2.14)$$

Furthermore, $\partial\mathcal{D} = \Gamma_D \cup \Gamma_N$ with $\Gamma_D \cap \Gamma_N = \emptyset$, where Γ_D and Γ_N are respectively Dirichlet and Neumann boundaries. Thus, $\overline{u}$ is prescribed displacement on Γ_D and $\overline{q}$ is prescribed traction on Γ_N. Finally, p is a given hydrostatic pressure assumed to be constant in $\omega \subset \mathcal{D}$. See Figure 2. The strong formulation associated with the variational problem (2.8) is given by: Find u, such that:

$$\left\{\begin{array}{rcll} \mathrm{div}\sigma(u) & = & 0 & \text{in } \mathcal{D}, \\ \sigma(u) & = & \rho\mathbb{C}\nabla u^s, & \\ u & = & \overline{u} & \text{on } \Gamma_D, \\ \sigma(u)n & = & \overline{q} & \text{on } \Gamma_N, \\ [\![u]\!] & = & 0 & \\ [\![\sigma(u)]\!]\, n & = & -pn & \end{array}\right\} \text{on } \partial\omega, \quad (2.15)$$

where the operator $[\![\varphi]\!]$ is used to denote the jump of the function φ on the interface $\partial\omega$, namely $[\![\varphi]\!] = \varphi_{|\Omega} - \varphi_{|\omega}$ on $\partial\omega$. The transmission condition on the interface $\partial\omega$ comes out from the variational formulation (2.8).

The topological perturbation we are dealing with consists in nucleating a small inclusion with non-homogeneous transmission condition on its interface. Such a topological perturbation is called *pressurized inclusion*.

Let us introduce the topologically perturbed counterpart of the problem we are dealing with. The idea consists in nucleating a circular inclusion, denoted by $B_\varepsilon(\hat{x})$, of radius ε and center at the arbitrary point $\hat{x} \in \mathcal{D}$, such that $\overline{B_\varepsilon(\hat{x})} \subset \mathcal{D}$. We assume that $B_\varepsilon(\hat{x})$ is submitted to a hydrostatic pressure loading, which leads to a non-homogeneous transmission condition on the interface $\partial B_\varepsilon(\hat{x})$. See sketch in Figure 3. In this case $\chi_\varepsilon(\hat{x})$ in defined as follows:

$$\chi_\varepsilon(\hat{x}) = \mathbb{1}_{\mathcal{D}} - (1-\gamma)\mathbb{1}_{B_\varepsilon(\hat{x})}, \quad (2.16)$$

where $\gamma = \gamma(x)$ is the contrast in the material properties. From these elements, we define a piecewise constant function of the form

$$\gamma_\varepsilon = \gamma_\varepsilon(x) := \begin{cases} 1 & \text{if } x \in \mathcal{D} \setminus \overline{B_\varepsilon}, \\ \gamma & \text{if } x \in B_\varepsilon. \end{cases} \quad (2.17)$$

The shape functional associated with the topologically perturbed problem is denoted by $\mathcal{J}_{\chi_\varepsilon}(u_\varepsilon)$, where

$$\mathcal{J}_{\chi_\varepsilon}(u_\varepsilon) = \frac{1}{2}\int_{\mathcal{D}} \sigma_\varepsilon(u_\varepsilon)\cdot\nabla u_\varepsilon^s - \int_{\Gamma_N} \overline{q}\cdot u_\varepsilon - \int_\omega p\,\mathrm{div}(u_\varepsilon) - \kappa\int_{B_\varepsilon} p\,\mathrm{div}(u_\varepsilon), \quad (2.18)$$

with the vector function u_ε solution of the following variational problem: Find $u_\varepsilon \in \mathcal{U}$, such that

$$\int_{\mathcal{D}} \sigma_\varepsilon(u_\varepsilon)\cdot\nabla\eta^s = \int_{\Gamma_N}\overline{q}\cdot\eta + \int_\omega p\,\mathrm{div}(\eta) + \kappa\int_{B_\varepsilon} p\,\mathrm{div}(\eta),\ \forall\eta\in\mathcal{V}. \quad (2.19)$$

Some terms in the above equation require explanation. The Cauchy stress tensor $\sigma_\varepsilon(u_\varepsilon) = \gamma_\varepsilon\sigma(u_\varepsilon)$, where γ_ε is given by (2.17). The hydrostatic pressure is denoted by p. The parameter κ is introduced to control whether the topological perturbation B_ε is

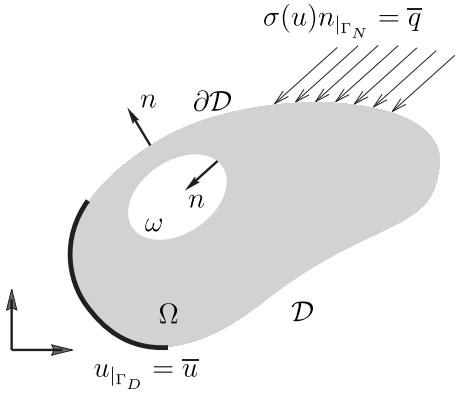

FIGURE 2. Unperturbed problem.

nucleated either in Ω or in ω, namely

$$\kappa = \kappa(x) := \begin{cases} +1 & \text{if } x \in \Omega, \\ -1 & \text{if } x \in \omega. \end{cases} \tag{2.20}$$

The strong formulation associated with the variational problem (2.19) is given by: Find u_ε, such that:

$$\begin{cases} \operatorname{div}\sigma_\varepsilon(u_\varepsilon) = 0 & \text{in } \mathcal{D}, \\ \sigma_\varepsilon(u_\varepsilon) = \gamma_\varepsilon\sigma(u_\varepsilon), & \\ u_\varepsilon = \overline{u} & \text{on } \Gamma_D, \\ \sigma(u_\varepsilon)n = \overline{q} & \text{on } \Gamma_N, \\ \left.\begin{array}{rcl} [\![u_\varepsilon]\!] &=& 0 \\ [\![\sigma_\varepsilon(u_\varepsilon)]\!]\, n &=& -pn \end{array}\right\} & \text{on } \partial\omega. \\ \left.\begin{array}{rcl} [\![u_\varepsilon]\!] &=& 0 \\ [\![\sigma_\varepsilon(u_\varepsilon)]\!]\, n &=& -\kappa pn \end{array}\right\} & \text{on } \partial B_\varepsilon. \end{cases} \tag{2.21}$$

The transmission conditions on the interfaces $\partial\omega$ and ∂B_ε come out from the variational formulation (2.19).

2.2. **Existence of the Topological Derivative.** The existence of the topological derivative is ensured by the following result:

Lemma 1. *Let u_ε and u be solutions of problems (2.21) and (2.15), respectively. Then, the following estimate holds true:*

$$\|u_\varepsilon - u\|_{H^1(\mathcal{D})} \leq C\varepsilon, \tag{2.22}$$

where C is a constant independent of the small parameter ε.

Proof. Let us subtract (2.8) from (2.19). Then, from the definition to the contrast (2.17), we obtain

$$\begin{aligned} \kappa \int_{B_\varepsilon} p \operatorname{div}(\eta) &= \int_{\mathcal{D}} (\sigma_\varepsilon(u_\varepsilon) - \sigma(u)) \cdot \nabla\eta^s \\ &= \int_{\mathcal{D}\setminus B_\varepsilon} (\sigma(u_\varepsilon) - \sigma(u)) \cdot \nabla\eta^s \\ &\quad + \int_{B_\varepsilon} (\gamma\sigma(u_\varepsilon) - \sigma(u)) \cdot \nabla\eta^s. \end{aligned} \tag{2.23}$$

After adding and subtracting the term

$$\int_{B_\varepsilon} \gamma\sigma(u) \cdot \nabla\eta^s \tag{2.24}$$

in the above expression we have:

$$\begin{aligned} \kappa \int_{B_\varepsilon} p \operatorname{div}(\eta) = \int_{\mathcal{D}} \sigma_\varepsilon(u_\varepsilon - u) \cdot \nabla\eta^s \\ + \int_{B_\varepsilon} (\gamma - 1)\sigma(u) \cdot \nabla\eta^s. \end{aligned} \tag{2.25}$$

By taking $\eta = u_\varepsilon - u$ as test function in (2.25) we obtain the following equality:

$$\begin{aligned} &\int_{\mathcal{D}} \sigma_\varepsilon(u_\varepsilon - u) \cdot \nabla(u_\varepsilon - u)^s = \\ &\int_{B_\varepsilon} (1 - \gamma)\sigma(u) \cdot \nabla(u_\varepsilon - u)^s + \\ &\kappa \int_{B_\varepsilon} p \operatorname{div}(u_\varepsilon - u). \end{aligned} \tag{2.26}$$

From the above expression, we have

$$\begin{aligned} &\int_{\mathcal{D}} \sigma_\varepsilon(u_\varepsilon - u) \cdot \nabla(u_\varepsilon - u)^s = \\ &\int_{B_\varepsilon} T(u) \cdot \nabla(u_\varepsilon - u)^s, \end{aligned} \tag{2.27}$$

where we have introduced the notation

$$\mathrm{T}(u) = (1 - \gamma)\sigma(u) + \kappa p\mathrm{I}. \tag{2.28}$$

From the Cauchy-Schwarz inequality it follows that

$$\begin{aligned} &\int_{\mathcal{D}} \sigma_\varepsilon(u_\varepsilon - u) \cdot \nabla(u_\varepsilon - u)^s \leq \\ &\|\mathrm{T}(u)\|_{L^2(B_\varepsilon)} \|\nabla(u_\varepsilon - u)\|_{L^2(B_\varepsilon)} \leq \\ &c_0\varepsilon \|\nabla(u_\varepsilon - u)\|_{L^2(B_\varepsilon)} \leq c_1\varepsilon \|u_\varepsilon - u\|_{H^1(\mathcal{D})}. \end{aligned} \tag{2.29}$$

From the coercivity of the bilinear form on the left-hand side of (2.29) we have

$$c\|u_\varepsilon - u\|^2_{H^1(\mathcal{D})} \leq \int_{\mathcal{D}} \sigma_\varepsilon(u_\varepsilon - u) \cdot \nabla(u_\varepsilon - u)^s, \tag{2.30}$$

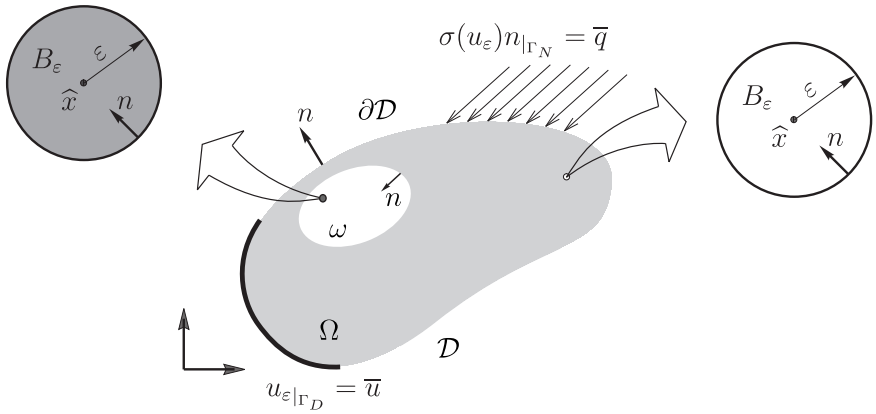

FIGURE 3. Perturbed problem.

which leads to the result with $C = c_1/c$ independent of the small parameter ε. □

2.3. **The Topological Derivative Formula.** The topological derivative of the volume constraint is trivially obtained and given by

$$D_T|\Omega|(x) = \kappa(x)\, m, \quad \forall x \in \mathcal{D}, \tag{2.31}$$

where the signal function $\kappa(x)$ is defined in (2.20). In addition, according to Appendix A, the topological derivative of the energy shape functional is given by (A.35), with the polarization tensor defined through (A.36). Since we are using a very weak material to replace the voids, we can take the limit cases $\gamma \to 0$ and $\gamma \to \infty$ in (A.35). Formally, for $\gamma \to 0$ the inclusion represents a hole and the transmission condition on the boundary of the inclusion degenerates itself to non-homogeneous Neumann boundary condition. In this case the topological derivative evaluated within the elastic material Ω becomes

$$\begin{aligned} D_T\mathcal{J}_\chi(x) = &-\mathbb{P}_0\sigma(u)(x)\cdot\nabla u^s(x) \\ &-(1+\alpha)\, p\,\mathrm{div}(u)(x) \\ &-\frac{p^2}{2\mu}, \quad \forall x \in \Omega, \end{aligned} \tag{2.32}$$

with the polarization tensor given by

$$\mathbb{P}_0 = \frac{1+\beta}{2}\mathbb{I} + \frac{\alpha-\beta}{4}\mathrm{I}\otimes\mathrm{I}. \tag{2.33}$$

In addition, for $\gamma \to \infty$, the elastic inclusion leads to a rigid inclusion. In this case the topological derivative evaluated into the compliant material ω results in

$$D_T\mathcal{J}_\chi(x) = -\mathbb{P}_\infty\sigma(u)(x)\cdot\nabla u^s(x), \quad \forall x \in \omega, \tag{2.34}$$

where the polarization tensor is given by

$$\mathbb{P}_\infty = -\frac{1+\beta}{2\beta}\mathbb{I} + \frac{\alpha-\beta}{4\alpha\beta}\mathrm{I}\otimes\mathrm{I}. \tag{2.35}$$

The coefficients α and β are defined through (A.37). Finally, the topological derivative of the shape functional (2.6) is given by the sum

$$D_T\mathcal{F}_\chi(x) = D_T\mathcal{J}_\chi(x) + D_T|\Omega|(x), \quad \forall x \in \mathcal{D}. \tag{2.36}$$

3. Numerical Results

The minimization problem (2.6) is solved by using an efficient algorithm proposed by Amstutz and Andrä (2006). It is based on the topological derivative concept and a level-set domain representation method and has been applied in many different problems, see for instance, Amigo et al. (2016); Amstutz et al. (2010); Amstutz and Novotny (2010); Amstutz et al. (2012); Mróz et al. (2017); Sá et al. (2016); Torii et al. (2016). For further explanations of this algorithm, see Amstutz (2011). See also Lopes et al. (2015), where the algorithm is presented in a pseudo-code format.

In all numerical examples the material properties are set as: Young's modulus $E = 1.0$, Poisson's ratio $\nu = 0.3$ and contrast $\rho_0 = 10^{-4}$. The topology is identified by the elastic material distribution and the compliant material is used to mimic voids. Since we are dealing with design-dependent hydrostatic pressure loads, the region ω remains pressurized during all optimization process. The mechanical problem is discretized into linear triangular finite elements and three steps of uniform mesh refinement were performed during the iterative process. We assume that in the first and in the last examples the structures are under plane stress assumption while in the second example the structure is under plane strain assumption.

3.1. **Example 1.** In this first example, the hold-all domain $\mathcal{D}$ consists in a rectangle of size 1.0×0.7 as shown in Figure 4(a). The initial pressurized region ω is confined in a smaller rectangle of size 1.0×0.1.

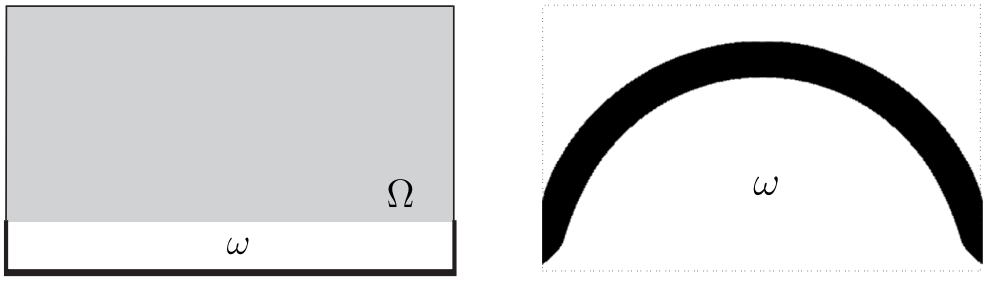

(a) initial guess (b) final result

FIGURE 4. Example 1.

The thick lines are used to represent clamped boundary condition. The hydrostatic pressure loading and the penalty parameter are set as $p = 1$ and $m = 5$, respectively. The initial mesh used to discretize the domain $\mathcal{D}$ has 3840 elements and 1985 nodes, while the final mesh has 245760 elements and 123393 nodes. The final result is obtained after 46 iterations and contains 22% of the initial volume, as shown in Figure 4(b). We observe that the pressurized region remains confined under the resulting arc-tie structure. The convergence of the shape functional $\mathcal{F}_\chi(u)$ is presented in Figure 5. Similar results has been found by Hammer and Olhoff (2000) and Wang et al. (2016), for instance.

3.2. **Example 2.** In this example, the hold-all domain $\mathcal{D}$ is given by a unit square cross-section of a prismatic bar as shown in Figure 6(a). The pressurized region ω is confined into a smaller square of size 0.5×0.5. The dashed-dotted lines are used to denote symmetry conditions. The initial mesh has 6400 elements and 3281 nodes, while the final mesh has 409600 elements and 205441 nodes. The hydrostatic pressure loading and the penalty parameter are set as $p = 1$ and $m = 0.2$, respectively. The final result, shown in Figure 6(b), is obtained after 49 iterations and contains 81% of the initial volume. This result can be interpreted as the optimal cross-section of a pipe submitted to internal hydrostatic pressure loading, for instance.

3.3. **Example 3.** In this last example, the hold-all domain $\mathcal{D}$ is given by a square of size 1.0×1.0, which is submitted to a horizontal load $\overline{q}$ applied on the middle top of the square. The thick line represents clamped boundary condition. The pressurized region ω is confined into a semicircle of radius $r = 0.4$ and center at the middle bottom of the square. See Figure 7. The penalty parameter is set as $m = 0.2$. The initial mesh has 6400 elements and 3281 nodes, while the final mesh has 409600 elements and 205441 nodes. The obtained results for different combinations of $\overline{q}$ and p are presented in Figure 8, namely $p = 1.0$ and $\overline{q} = (0, 0)$, $p = 0$ and $\overline{q} = (1, 0)$, $p = 2.0$ and $\overline{q} = (1, 0)$, and finally $p = 5.0$ and $\overline{q} = (1, 0)$. It is interesting to note from Figures 8(c) and 8(d) that there is a changing in the curvature of the right leg of the structure after increasing the hydrostatic pressure loading from $p = 2.0$ to $p = 5.0$.

4. Conclusion

In this paper a new methodology dealing with topology optimization of structures subject to design-dependent hydrostatic pressure loading has been presented. In particular, the structural compliance is minimized under volume constraint. The associated topological derivative with respect to the nucleation of a circular inclusion subject to non-homogeneous transmission condition has been rigorously obtained, which represents the main contribution of this paper. In addition, the obtained result has been used in a topology optimization algorithm based on the associated topological derivative together with a level-set domain representation method. The strikingly simplicity of the proposed methodology should be noted. In fact, since the hydrostatic pressure loading comes out naturally from the variational formulation, just a minimal number of user-defined algorithmic parameters is required. Finally, some numerical examples were presented, showing the influence of the hydrostatic pressure on the topology of the structure. The numerical examples agree well with the results that should be expected by other methods. Therefore, our approach can be seen as a simple alternative method for compliance topology optimization of structures subject to design-dependent hydrostatic pressure loading under volume constraint.

Acknowledgements

This research was partly supported by CNPq (Brazilian Research Council), CAPES (Brazilian

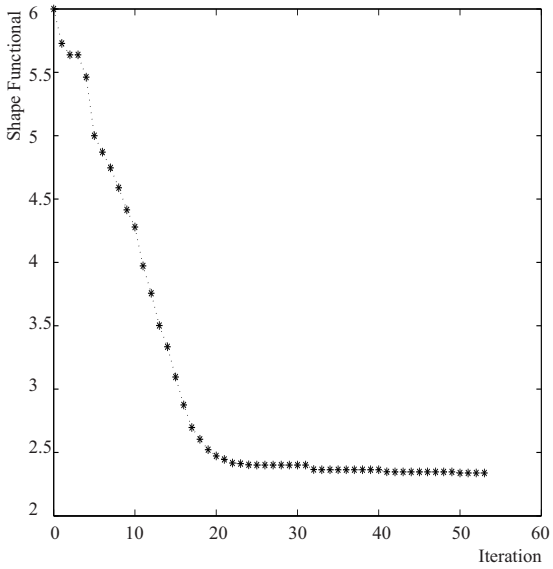

FIGURE 5. Example 1: History of the shape functional $\mathcal{F}_\chi(u)$ values.

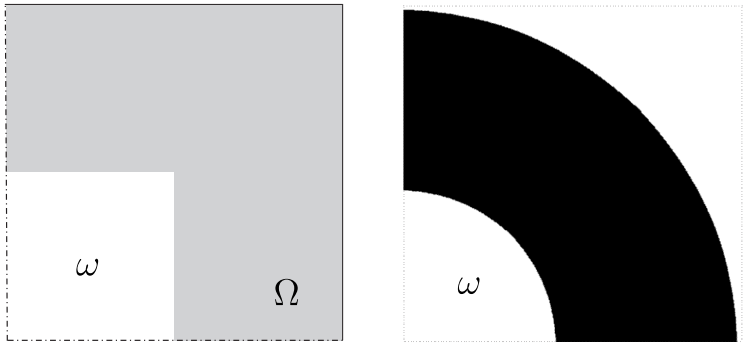

(a) initial guess (b) final result

FIGURE 6. Example 2.

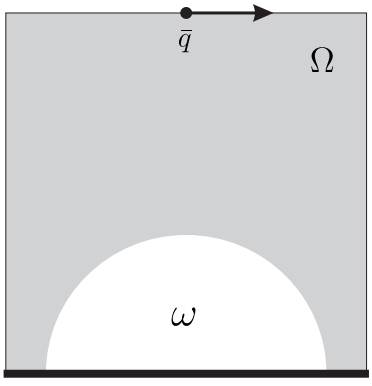

FIGURE 7. Example 3: Initial guess.

Higher Education Staff Training Agency) and FAPERJ (Research Foundation of the State of Rio de Janeiro). These supports are gratefully acknowledged.

APPENDIX A. TOPOLOGICAL DERIVATIVE EVALUATION

In order to evaluate the difference between the functionals $\mathcal{J}_\chi(u)$ and $\mathcal{J}_{\chi_\varepsilon}(u_\varepsilon)$, respectively defined in (2.7) and (2.18), we start by taking $\eta = u_\varepsilon - u$ as

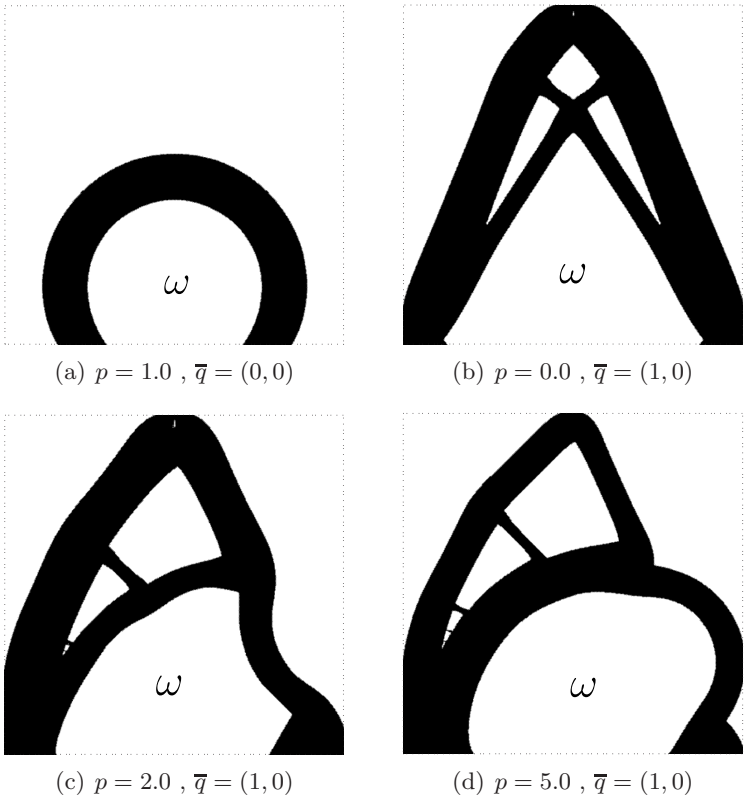

(a) $p = 1.0$, $\overline{q} = (0, 0)$ (b) $p = 0.0$, $\overline{q} = (1, 0)$

(c) $p = 2.0$, $\overline{q} = (1, 0)$ (d) $p = 5.0$, $\overline{q} = (1, 0)$

FIGURE 8. Example 3: Final results.

test function in the variational problem (2.8). Then we have the following equality

$$\begin{aligned}\int_{\mathcal{D}} \sigma(u) \cdot \nabla u^s = &\int_{\mathcal{D}} \sigma(u) \cdot \nabla u_\varepsilon^s \\ &- \int_{\Gamma_N} \overline{q} \cdot (u_\varepsilon - u) \\ &- \int_{\omega} p \operatorname{div}(u_\varepsilon - u). \end{aligned} \tag{A.1}$$

After replacing (A.1) into (2.7) we obtain

$$\begin{aligned}\mathcal{J}_\chi(u) = &\frac{1}{2}\int_{\mathcal{D}} \sigma(u) \cdot \nabla u_\varepsilon^s \\ &- \frac{1}{2}\int_{\Gamma_N} \overline{q} \cdot (u_\varepsilon + u) \\ &- \frac{1}{2}\int_{\omega} p \operatorname{div}(u_\varepsilon + u). \end{aligned} \tag{A.2}$$

In the same way, let us set $\eta = u_\varepsilon - u$ as test function in the variational problem (2.19). Thus

$$\begin{aligned}\int_{\mathcal{D}} \sigma_\varepsilon(u_\varepsilon) \cdot \nabla u_\varepsilon^s = &\int_{\mathcal{D}} \sigma_\varepsilon(u_\varepsilon) \cdot \nabla u^s \\ &+ \int_{\Gamma_N} \overline{q} \cdot (u_\varepsilon - u) \\ &+ \int_{\omega} p \operatorname{div}(u_\varepsilon - u) \\ &+ \kappa \int_{B_\varepsilon} p \operatorname{div}(u_\varepsilon - u). \end{aligned} \tag{A.3}$$

After replacing (A.3) into (2.18), it follows

$$\begin{aligned}\mathcal{J}_{\chi_\varepsilon}(u_\varepsilon) = &\frac{1}{2}\int_{\mathcal{D}} \sigma_\varepsilon(u_\varepsilon) \cdot \nabla u^s \\ &- \frac{1}{2}\int_{\Gamma_N} \overline{q} \cdot (u_\varepsilon + u) \\ &- \frac{1}{2}\int_{\omega} p \operatorname{div}(u_\varepsilon + u) \\ &- \frac{1}{2}\kappa \int_{B_\varepsilon} p \operatorname{div}(u_\varepsilon + u). \end{aligned} \tag{A.4}$$

From (A.2) and (A.4), the variation of the energy shape functionals can be written as

$$\mathcal{J}_{\chi_\varepsilon}(u_\varepsilon) - \mathcal{J}_\chi(u) = \frac{1}{2}\int_{\mathcal{D}} \sigma_\varepsilon(u_\varepsilon)\cdot\nabla u^s - \frac{1}{2}\int_{\mathcal{D}} \sigma(u_\varepsilon)\cdot\nabla u^s - \frac{1}{2}\kappa\int_{B_\varepsilon} p\,\mathrm{div}(u_\varepsilon + u). \quad (A.5)$$

Now, by taking into account the definition for the contrast γ_ε given by (2.17), we have

$$\mathcal{J}_{\chi_\varepsilon}(u_\varepsilon) - \mathcal{J}_\chi(u) = \frac{1}{2}\int_{\mathcal{D}\setminus B_\varepsilon} \sigma(u_\varepsilon)\cdot\nabla u^s + \frac{1}{2}\int_{B_\varepsilon} \gamma\sigma(u_\varepsilon)\cdot\nabla u^s - \frac{1}{2}\int_{\mathcal{D}\setminus B_\varepsilon} \sigma(u_\varepsilon)\cdot\nabla u^s - \frac{1}{2}\int_{B_\varepsilon} \sigma(u_\varepsilon)\cdot\nabla u^s - \frac{1}{2}\kappa\int_{B_\varepsilon} p\,\mathrm{div}(u_\varepsilon + u). \quad (A.6)$$

Let us add and subtract the term

$$\frac{1}{2}\kappa\int_{B_\varepsilon} p\,\mathrm{div}(u). \quad (A.7)$$

Thus, the following expression is obtained after canceling the identical terms

$$\mathcal{J}_{\chi_\varepsilon}(u_\varepsilon) - \mathcal{J}_\chi(u) = \int_{B_\varepsilon} \frac{\gamma-1}{2\gamma}\sigma_\varepsilon(u_\varepsilon)\cdot\nabla u^s - \kappa\int_{B_\varepsilon} p\,\mathrm{div}(u) - \frac{1}{2}\kappa\int_{B_\varepsilon} p\,\mathrm{div}(u_\varepsilon - u). \quad (A.8)$$

Note that the variation of the energy shape functional results in an integral concentrated into the inclusion B_ε. Therefore, in order to apply the definition for the topological derivative given by (2.2), we need to know the asymptotic behavior of the function u_ε with respect the small parameter ε. Thus, let us introduce the following ansätz:

$$u_\varepsilon = u + w_\varepsilon + \tilde{u}_\varepsilon, \quad (A.9)$$

where u is solution of the unperturbed problem (2.7), w_ε is solution to an auxiliary exterior problem and $\tilde{u}_\varepsilon$ is the remainder.

After applying the operator σ_ε in the ansätz (A.9) we have

$$\sigma_\varepsilon(u_\varepsilon) = \sigma_\varepsilon(u) + \sigma_\varepsilon(w_\varepsilon) + \sigma_\varepsilon(\tilde{u}_\varepsilon). \quad (A.10)$$

By expanding $\sigma(u)$ in Taylor's series around the point $\hat{x}$ we obtain

$$\sigma_\varepsilon(u_\varepsilon) = \sigma_\varepsilon(u)(\hat{x}) + \gamma_\varepsilon\nabla\sigma(u(\xi))(x-\hat{x}) + \sigma_\varepsilon(w_\varepsilon) + \sigma_\varepsilon(\tilde{u}_\varepsilon), \quad (A.11)$$

where ξ is an intermediate point between x and $\hat{x}$. On the boundary of the inclusion B_ε we have

$$[\![\sigma_\varepsilon(u_\varepsilon)]\!]n = -\kappa p n. \quad (A.12)$$

After evaluating (A.12) we obtain

$$(\sigma(u_\varepsilon)_{|_{\mathcal{D}\setminus\overline{B_\varepsilon}}} - \gamma\sigma(u_\varepsilon)_{|_{B_\varepsilon}})n = -\kappa p n \quad \text{on} \quad \partial B_\varepsilon. \quad (A.13)$$

Then, let us evaluate (A.11) on ∂B_ε to have

$$-\kappa p n = (1-\gamma)\sigma(u)(\hat{x})n - \varepsilon(1-\gamma)(\nabla\sigma(u(\xi))n)n + [\![\sigma_\varepsilon(w_\varepsilon)]\!]n + [\![\sigma_\varepsilon(\tilde{u}_\varepsilon)]\!]n, \quad (A.14)$$

since $(x-\hat{x}) = -\varepsilon n$ on ∂B_ε. By choosing $\sigma_\varepsilon(w_\varepsilon)$ such as

$$[\![\sigma_\varepsilon(w_\varepsilon)]\!]n = ((\gamma-1)\sigma(u)(\hat{x}) - \kappa p\mathrm{I})n \quad \text{on} \quad \partial B_\varepsilon, \quad (A.15)$$

the following auxiliary boundary value problem is considered and formally obtained when $\varepsilon \to 0$: Find $\sigma_\varepsilon(w_\varepsilon)$ such that:

$$\begin{cases} \mathrm{div}\sigma_\varepsilon(w_\varepsilon) = 0 & \text{in} \quad \mathbb{R}^2, \\ \sigma_\varepsilon(w_\varepsilon) \to 0 & \text{in} \quad \infty, \\ [\![\sigma_\varepsilon(w_\varepsilon)]\!]\,n = \hat{u} & \text{on} \quad \partial B_\varepsilon, \end{cases} \quad (A.16)$$

with $\hat{u} = ((\gamma-1)\sigma(u)(\hat{x}) - \kappa p\mathrm{I})n$. The boundary value problem (A.16) admits an explicit solution. For $p = 0$, its solution can be found in (Novotny and Sokołowski, 2013, Ch. 5, pp. 156), for instance. Since the stress $\sigma_\varepsilon(w_\varepsilon)$ is uniform inside the inclusion, the solution of (A.16) for $p \neq 0$ can be written in a following compact form

$$\sigma_\varepsilon(w_\varepsilon)_{|_{B_\varepsilon}} = \mathbb{T}_\gamma\sigma(u)(\hat{x}) + \mathrm{T}_\gamma, \quad (A.17)$$

where $\mathbb{T}_\gamma$ is a fourth order isotropic tensor given by

$$\mathbb{T}_\gamma = \frac{\gamma(1-\gamma)}{2(1+\beta\gamma)}\left(2\beta\mathbb{I} + \frac{\alpha-\beta}{1+\alpha\gamma}\mathrm{I}\otimes\mathrm{I}\right) \quad (A.18)$$

and T_γ is a second order isotropic tensor written as

$$\mathrm{T}_\gamma = \kappa p\frac{\alpha\gamma}{1+\alpha\gamma}\mathrm{I}. \quad (A.19)$$

The result shown in (A.17) fits the famous Eshelby's problem. This problem, formulated by Eshelby (1957, 1959), represents one of the major advances in the continuum mechanics theory of the 20$^{\text{th}}$ century (Kachanov et al., 2003).

Now we can construct $\sigma_\varepsilon(\tilde{u}_\varepsilon)$ in such a way that it compensates for the discrepancies introduced by the higher-order terms in ε as well as by the boundary-layer w_ε on the exterior boundary $\partial\mathcal{D}$. It means that the remainder $\tilde{u}_\varepsilon$ must be solution to the following boundary value problem: Find $\tilde{u}_\varepsilon$ such that:

$$\left\{\begin{array}{rcll} \mathrm{div}\sigma_\varepsilon(\tilde{u}_\varepsilon) &=& 0 & \text{in } \mathcal{D},\\ \sigma_\varepsilon(\tilde{u}_\varepsilon) &=& \gamma_\varepsilon\sigma(\tilde{u}_\varepsilon), & \\ \tilde{u}_\varepsilon &=& -w_\varepsilon & \text{on } \Gamma_D,\\ \sigma(\tilde{u}_\varepsilon)n &=& -\sigma(w_\varepsilon)n & \text{on } \Gamma_N,\\ [\![\sigma_\varepsilon(\tilde{u}_\varepsilon)]\!]\, n &=& 0 & \text{on } \partial\omega,\\ [\![\tilde{u}_\varepsilon]\!] &=& 0 & \text{on } \partial B_\varepsilon\\ [\![\sigma_\varepsilon(\tilde{u}_\varepsilon)]\!]\, n &=& \varepsilon h & \end{array}\right. \tag{A.20}$$

with $h = (1-\gamma)(\nabla\sigma(u(\xi))n)n$. The estimate $\|\tilde{u}_\varepsilon\|_{H^1(\mathcal{D})} = O(\varepsilon^2)$ for the remainder $\tilde{u}_\varepsilon$ holds true. See, for instance, the book by (Novotny and Sokołowski, 2013, Ch. 5, pp 155).

From the above results, we can evaluate the integrals in (A.8) explicitly. In fact, after replacing the ansätz for u_ε given by (A.9) in the first integral of (A.8) we have

$$\begin{aligned}\int_{B_\varepsilon}\sigma_\varepsilon(u_\varepsilon)\cdot\nabla u^s = &\underbrace{\int_{B_\varepsilon}\sigma_\varepsilon(u)\cdot\nabla u^s}_{(a)}\\ &+\underbrace{\int_{B_\varepsilon}\sigma_\varepsilon(w_\varepsilon)\cdot\nabla u^s}_{(b)}\\ &+\mathcal{E}_1(\varepsilon).\end{aligned} \tag{A.21}$$

The remainder $\mathcal{E}_1(\varepsilon)$ is given by

$$\begin{aligned}\mathcal{E}_1(\varepsilon) &= \int_{B_\varepsilon}\sigma_\varepsilon(\tilde{u}_\varepsilon)\cdot\nabla u^s\\ &\le \|\sigma_\varepsilon(\tilde{u}_\varepsilon)\|_{L^2(B_\varepsilon)}\|\nabla u\|_{L^2(B_\varepsilon)}\\ &\le c_1\|\tilde{u}_\varepsilon\|_{H^1(\mathcal{D})}\|\nabla u\|_{L^2(B_\varepsilon)}\\ &\le c_2\varepsilon^3 = O(\varepsilon^3),\end{aligned} \tag{A.22}$$

where we have used the Cauchy-Schwarz inequality together with the estimation for the remainder $\tilde{u}_\varepsilon$. The term (a) in (A.21) can be developed in power of ε as follows

$$\begin{aligned}\int_{B_\varepsilon}\sigma_\varepsilon(u)\cdot\nabla u^s &= \int_{B_\varepsilon}\gamma\sigma(u)\cdot\nabla u^s\\ &= \pi\varepsilon^2\gamma\sigma(u)(\hat{x})\cdot\nabla u^s(\hat{x})\\ &+\mathcal{E}_2(\varepsilon),\end{aligned} \tag{A.23}$$

with the remainder $\mathcal{E}_2(\varepsilon)$ defined as

$$\begin{aligned}\mathcal{E}_2(\varepsilon) &= \int_{B_\varepsilon}(h(x)-h(\hat{x}))\\ &\le \|h(x)-h(\hat{x})\|_{L^2(B_\varepsilon)}\|1\|_{L^2(B_\varepsilon)}\\ &\le c_1\varepsilon\|x-\hat{x}\|_{L^2(B_\varepsilon)} \le c_2\varepsilon^3 = O(\varepsilon^3),\end{aligned} \tag{A.24}$$

where we have introduced the notation

$$\begin{aligned}&h(x)-h(\hat{x}) =\\ &\sigma(u)(x)\cdot\nabla u^s(x) - \sigma(u)(\hat{x})\cdot\nabla u^s(\hat{x}).\end{aligned} \tag{A.25}$$

Note that, we have used again the Cauchy-Schwarz inequality and the interior elliptic regularity of function u. Since the exact solution of the auxiliary problem (A.16) is known, the term (b) in (A.21) can be written as

$$\begin{aligned}&\int_{B_\varepsilon}\sigma_\varepsilon(w_\varepsilon)\cdot\nabla u^s =\\ &\pi\varepsilon^2\nabla u^s(\hat{x})\cdot(\mathbb{T}_\gamma\sigma(u)(\hat{x})+\mathrm{T}_\gamma)+\mathcal{E}_3(\varepsilon).\end{aligned} \tag{A.26}$$

The remainder $\mathcal{E}_3(\varepsilon)$ is given by

$$\begin{aligned}\mathcal{E}_3(\varepsilon) &= \int_{B_\varepsilon}\sigma_\varepsilon(w_\varepsilon)\cdot(\nabla u^s-\nabla u^s(\hat{x}))\\ &\le \|\sigma_\varepsilon(w_\varepsilon)\|_{L^2(B_\varepsilon)}\|\nabla u-\nabla u(\hat{x})\|_{L^2(B_\varepsilon)}\\ &\le c_1\varepsilon\|x-\hat{x}\|_{L^2(B_\varepsilon)} \le c_2\varepsilon^3 = O(\varepsilon^3),\end{aligned} \tag{A.27}$$

where we have used again the Cauchy-Schwarz inequality and the interior elliptic regularity of function u.

The second term in (A.8) can be developed as follows

$$\kappa\int_{B_\varepsilon}p\,\mathrm{div}(u) = \pi\varepsilon^2\kappa p\,\mathrm{div}(u)(\hat{x})+\mathcal{E}_4(\varepsilon), \tag{A.28}$$

where the remainder $\mathcal{E}_4(\varepsilon)$ is defined as

$$\begin{aligned}\mathcal{E}_4(\varepsilon) &= \kappa\int_{B_\varepsilon}p(\mathrm{div}(u)-\mathrm{div}(u)(\hat{x}))\\ &\le c_1\|x-\hat{x}\|_{L^2(B_\varepsilon)}\|1\|_{L^2(B_\varepsilon)}\\ &\le c_2\varepsilon^3 = O(\varepsilon^3).\end{aligned} \tag{A.29}$$

Once again, we have used the Cauchy-Schwarz inequality together with the interior elliptic regularity of function u.

After replacing the ansätz for u_ε given by (A.9) into the last term of (A.8) we have

$$\begin{aligned}\frac{1}{2}\kappa\int_{B_\varepsilon}p\,\mathrm{div}(u_\varepsilon-u) &= \frac{1}{2}\kappa\int_{B_\varepsilon}p\,\mathrm{div}(w_\varepsilon+\tilde{u}_\varepsilon)\\ &= \frac{1}{2}\kappa\int_{B_\varepsilon}p\,\mathrm{div}(w_\varepsilon)\\ &+\mathcal{E}_5(\varepsilon).\end{aligned} \tag{A.30}$$

where the remainder $\mathcal{E}_5(\varepsilon)$ has the following bound thanks to the estimate for $\tilde{u}_\varepsilon$

$$\begin{aligned}\mathcal{E}_5(\varepsilon) &= \frac{1}{2}\kappa \int_{B_\varepsilon} p\,\mathrm{div}(\tilde{u}_\varepsilon) \\ &\leq c_1 \|\nabla \tilde{u}_\varepsilon\|_{L^2(B_\varepsilon)} \|1\|_{L^2(B_\varepsilon)} \\ &\leq c_2 \varepsilon \|\tilde{u}_\varepsilon\|_{H^1(\mathcal{D})} \leq c_2 \varepsilon^3 = O(\varepsilon^3). \end{aligned} \tag{A.31}$$

By using the constitutive relation and after algebraic manipulations, we have

$$\begin{aligned}&\frac{1}{2}\kappa \int_{B_\varepsilon} p\,\mathrm{div}(w_\varepsilon) = \\ &\frac{1}{2}\kappa \int_{B_\varepsilon} \frac{p}{2\gamma\rho(\mu+\lambda)} \mathrm{tr}\sigma_\varepsilon(w_\varepsilon), \end{aligned} \tag{A.32}$$

where $\mathrm{tr}\sigma_\varepsilon(w_\varepsilon)$, evaluated inside the inclusion, is given by

$$\begin{aligned}&\mathrm{tr}\sigma_\varepsilon(w_\varepsilon)_{|_{B_\varepsilon(\hat{x})}} = \\ &\frac{\alpha\gamma}{1+\alpha\gamma}((1-\gamma)\mathrm{tr}\sigma(u)(\hat{x}) + 2\kappa p). \end{aligned} \tag{A.33}$$

From the above results, the variation of the energy shape functionals, given by (A.8), can be developed in power of ε as follows

$$\begin{aligned}&\mathcal{J}_{\chi_\varepsilon}(u_\varepsilon) - \mathcal{J}_\chi(u) = \\ &-\pi\varepsilon^2 \frac{1-\gamma}{2\gamma} \left[\gamma\sigma(u)(\hat{x}) + (\mathbb{T}_\gamma \sigma(u)(\hat{x}) + \mathrm{T}_\gamma)\right] \cdot \nabla u^s(\hat{x}) \\ &-\pi\varepsilon^2 \kappa p\,\mathrm{div}(u)(\hat{x}) - \pi\varepsilon^2 \frac{\alpha}{2}\frac{1-\gamma}{1+\alpha\gamma}\kappa p\,\mathrm{div}(u)(\hat{x}) \\ &-\pi\varepsilon^2 \frac{p^2}{2\mu\rho(1+\alpha\gamma)} + \sum_{i=1}^{5} \mathcal{E}_i(\varepsilon), \end{aligned} \tag{A.34}$$

where the remainders $\mathcal{E}_i(\varepsilon) = o(\varepsilon^2)$, for $i = 1, ..., 5$, as previously shown. By defining the function $f(\varepsilon) = \pi\varepsilon^2$ and after applying the topological derivative concept in (A.34), we obtain

$$\begin{aligned}D_T \mathcal{J}_\chi(\hat{x}) = &-\mathbb{P}_\gamma \sigma(u)(\hat{x}) \cdot \nabla u^s(\hat{x}) \\ &- \frac{1+\alpha}{1+\alpha\gamma}\kappa p\,\mathrm{div}(u)(\hat{x}) \\ &- \frac{1}{2\rho\mu}\frac{p^2}{(1+\alpha\gamma)}, \end{aligned} \tag{A.35}$$

where $\mathbb{P}_\gamma$ is a fourth order isotropic tensor given by (Ammari and Kang, 2007)

$$\mathbb{P}_\gamma = \frac{1}{2}\frac{1-\gamma}{1+\beta\gamma}\left((1+\beta)\mathbb{I} + \frac{1}{2}(\alpha-\beta)\frac{1-\gamma}{1+\alpha\gamma}\mathrm{I}\otimes\mathrm{I}\right), \tag{A.36}$$

with the coefficients α and β defined as

$$\alpha = \frac{\lambda+\mu}{\mu} \quad \text{and} \quad \beta = \frac{\lambda+3\mu}{\lambda+\mu}. \tag{A.37}$$

References

R.C.R. Amigo, S.M. Giusti, A.A. Novotny, E.C.N. Silva, and J. Sokolowski. Optimum design of flextensional piezoelectric actuators into two spatial dimensions. *SIAM Journal on Control and Optimization*, 52(2):760–789, 2016.

H. Ammari and H. Kang. *Polarization and moment tensors with applications to inverse problems and effective medium theory*. Applied Mathematical Sciences vol. 162. Springer-Verlag, New York, 2007.

S. Amstutz. Analysis of a level set method for topology optimization. *Optimization Methods and Software*, 26(4-5):555–573, 2011.

S. Amstutz and H. Andrä. A new algorithm for topology optimization using a level-set method. *Journal of Computational Physics*, 216(2):573–588, 2006.

S. Amstutz and A. A. Novotny. Topological optimization of structures subject to von Mises stress constraints. *Structural and Multidisciplinary Optimization*, 41(3):407–420, 2010.

S. Amstutz, S. M. Giusti, A. A. Novotny, and E. A. de Souza Neto. Topological derivative for multiscale linear elasticity models applied to the synthesis of microstructures. *International Journal for Numerical Methods in Engineering*, 84:733–756, 2010.

S. Amstutz, A. A. Novotny, and E. A. de Souza Neto. Topological derivative-based topology optimization of structures subject to Drucker-Prager stress constraints. *Computer Methods in Applied Mechanics and Engineering*, 233–236:123–136, 2012.

D. E. Campeão, S. M. Giusti, and A. A. Novotny. Topology design of plates consedering different volume control methods. *Engineering Computations*, 31(5):826–842, 2014.

J. Céa, S. Garreau, Ph. Guillaume, and M. Masmoudi. The shape and topological optimizations connection. *Computer Methods in Applied Mechanics and Engineering*, 188(4):713–726, 2000.

B.C. Chen and N. Kikuchi. Topology optimization with design-dependent loads. *Finite Elements in Analysis and Design*, 37:57–70, 2001.

J. Du and N. Olhoff. Topological optimization of continuum structures with design-dependent surface loading - Part I: new computational approach for 2d problems. *Structural and Multidisciplinary Optimization*, 27(3):151–165, 2004a.

J. Du and N. Olhoff. Topological optimization of continuum structures with design-dependent surface loading - Part II: algorithm and examples for 3d problems. *Structural and Multidisciplinary Optimization*, 27(3):166–177, 2004b.

J. D. Eshelby. The determination of the elastic field of an ellipsoidal inclusion, and related problems. *Proceedings of the Royal Society: Section A*, 241: 376–396, 1957.

J. D. Eshelby. The elastic field outside an ellipsoidal inclusion, and related problems. *Proceedings of the Royal Society: Section A*, 252:561–569, 1959.

M.B. Fuchs and N.N.Y. Shemesh. Density-based topological design of structures subjected to water pressure using a parametric loading surface. *Structural and Multidisciplinary Optimization*, 28 (1):11–19, 2004.

T. Gao and W. Zhang. Topology optimization of multiphase-material structures under design dependent pressure loads. *International Journal for Simulation and Multidisciplinary Design Optimization*, 3:297–306, 2009.

S. Garreau, Ph. Guillaume, and M. Masmoudi. The topological asymptotic for PDE systems: the elasticity case. *SIAM Journal on Control and Optimization*, 39(6):1756–1778, 2001.

V.B. Hammer and N. Olhoff. Topology optimization of continuum structures subjected to pressure loading. *Structural and Multidisciplinary Optimization*, 19:85–92, 2000.

M. Kachanov, B. Shafiro, and I. Tsukrov. *Handbook of Elasticity Solutions*. Kluwer Academic Publishers, Dordrecht, 2003.

E. Lee and J.R.R.A. Martins. Structural topology optimization with design-dependent pressure loads. *Computer Methods in Applied Mechanics and Engineering*, 233-236:40–48, 2012.

C. G. Lopes, R. B. Santos, and A. A. Novotny. Topological derivative-based topology optimization of structures subject to multiple load-cases. *Latin American Journal of Solids and Structures*, 12: 834–860, 2015.

Z. Mróz, S. M. Giusti, J. Sokolowski, and A. A. Novotny. Topology design of thermomechanical actuators. *Structural and Multidisciplinary Optimization (to appear)*, pages 1–15, 2017.

J. A. Norato, M. P. Bendsøe, R. B. Haber, and D. Tortorelli. A topological derivative method for topology optimization. *Structural and Multidisciplinary Optimization*, 33(4–5):375–386, 2007.

A. A. Novotny and J. Sokołowski. *Topological derivatives in shape optimization*. Interaction of Mechanics and Mathematics. Springer-Verlag, Berlin, Heidelberg, 2013.

A. A. Novotny, R. A. Feijóo, C. Padra, and E. Taroco. Topological sensitivity analysis. *Computer Methods in Applied Mechanics and Engineering*, 192(7–8):803–829, 2003.

M.Y. Wang Q. Xia and T. Shi. Topology optimization with pressure load through a level set method. *Computer Methods in Applied Mechanics and Engineering*, 283:177–195, 2015.

L. F. N. Sá, R. C. R. Amigo, A. A. Novotny, and E. C. N. Silva. Topological derivatives applied to fluid flow channel design optimization problems. *Structural and Multidisciplinary Optimization*, 54 (2):249–264, 2016.

O. Sigmund and P.M. Clausen. Topology optimization using a mixed formulation: an alternative way to solve pressure load problems. *Computer Methods in Applied Mechanics and Engineering*, 196: 1874–1889, 2007.

J. Sokołowski and A. Żochowski. On the topological derivative in shape optimization. *SIAM Journal on Control and Optimization*, 37(4):1251–1272, 1999.

A. J. Torii, A. A. Novotny, and R. B. Santos. Robust compliance topology optimization based on the topological derivative concept. *International Journal for Numerical Methods in Engineering*, 106(11):889–903, 2016.

C. Wang, M. Zhao, and T. Ge. Structural topology optimization with design-dependent pressure loads. *Structural and Multidisciplinary Optimization*, 53(5):1005–1018, 2016.

(M. Xavier and A.A. Novotny) Laboratório Nacional de Computação Científica LNCC/MCT, Av. Getúlio Vargas 333, 25651-075 Petrópolis - RJ, Brasil.

E-mail address: marcel@lncc.br, novotny@lncc.br